



Targeted delivery of poly (methyl methacrylate) particles in colon cancer cells selectively attenuates cancer cell proliferation

Firdos Alam Khan, Sultan Akhtar, Dana Almohazey, Munther Alomari, Sarah Ameen Almofty, Ibrahim Badr, Abdelhamid Elaïssari

► To cite this version:

Firdos Alam Khan, Sultan Akhtar, Dana Almohazey, Munther Alomari, Sarah Ameen Almofty, et al.. Targeted delivery of poly (methyl methacrylate) particles in colon cancer cells selectively attenuates cancer cell proliferation. *Artificial Cells, Nanomedicine, and Biotechnology*, 2019, 47 (1), pp.1533-1542. 10.1080/21691401.2019.1577886 . hal-02989977

HAL Id: hal-02989977

<https://hal.science/hal-02989977>

Submitted on 16 Nov 2020

HAL is a multi-disciplinary open access archive for the deposit and dissemination of scientific research documents, whether they are published or not. The documents may come from teaching and research institutions in France or abroad, or from public or private research centers.

L'archive ouverte pluridisciplinaire **HAL**, est destinée au dépôt et à la diffusion de documents scientifiques de niveau recherche, publiés ou non, émanant des établissements d'enseignement et de recherche français ou étrangers, des laboratoires publics ou privés.

Targeted delivery of poly (methyl methacrylate) particles in colon cancer cells selectively attenuates cancer cell proliferation

Firdos Alam Khan, Sultan Akhtar, Dana Almohazey, Munther Alomari, Sarah Ameen Almoftly, Ibrahim Badr & Abdelhamid Elaissari

To cite this article: Firdos Alam Khan, Sultan Akhtar, Dana Almohazey, Munther Alomari, Sarah Ameen Almoftly, Ibrahim Badr & Abdelhamid Elaissari (2019) Targeted delivery of poly (methyl methacrylate) particles in colon cancer cells selectively attenuates cancer cell proliferation, *Artificial Cells, Nanomedicine, and Biotechnology*, 47:1, 1533-1542, DOI: [10.1080/21691401.2019.1577886](https://doi.org/10.1080/21691401.2019.1577886)

To link to this article: <https://doi.org/10.1080/21691401.2019.1577886>



© 2019 The Author(s). Published by Informa UK Limited, trading as Taylor & Francis Group.



Published online: 22 Apr 2019.



Submit your article to this journal [↗](#)



Article views: 1681



View related articles [↗](#)




View Crossmark data [↗](#)



Citing articles: 15 View citing articles [↗](#)

Targeted delivery of poly (methyl methacrylate) particles in colon cancer cells selectively attenuates cancer cell proliferation

Firdos Alam Khan^a , Sultan Akhtar^b, Dana Almohazey^a, Munther Alomari^a, Sarah Ameen Almoftay^a, Ibrahim Badr^c and Abdelhamid Elaissari^c

^aDepartment of Stem Cell Biology, Institute for Research and Medical Consultations, Imam Abdulrahman Bin Faisal University, Dammam, Saudi Arabia; ^bDepartment of Biophysics, Institute for Research and Medical Consultations, Imam Abdulrahman Bin Faisal University, Dammam, Saudi Arabia; ^cCentre national de la recherche scientifique, LAGEP-UMR 5007, University Claude Bernard Lyon-1, University of Lyon, Lyon, France

ABSTRACT

Poly (methyl methacrylate) (PMMA) is basically biocompatible polyester with high resistance to chemical hydrolysis, and high drug permeability and the most important characteristics of PMMA is that it does not produce any toxicity. There is not much information about PMMA action on the colon cancer cells. In the present study, we have synthesized PMMA nanoparticles. The distribution pattern of PMMA particles was analysed by Zeta sizer and the size of the particles was calculated by using quasi elastic light scattering (QELS). The surface structure and the morphology of PMMA were characterized by transmission electron microscope (TEM) and scanning electron microscope (SEM), respectively. We have also analysed their effects on cancerous cells (human colorectal carcinoma cells, HCT-116) and normal, healthy cells (human embryonic kidney cells, HEK-293) by using morphometric, MTT, DAPI and wound healing methods. We report that PMMA particles inhibited the cancer cell viability in a dose-dependent manner. The lower dose (1.0 µg/ml) showed a moderate decrease in cancer cell viability, whereas higher dosages (2.5 µg/ml, 5.0 µg/mL and 7.5 µg/mL) showed steadily decrease in the cancer cell viability. We also report that PMMA is highly selective to cancerous cells (HCT-116), as we did not find any action on the normal healthy cells (HEK-293). In conclusion, our results suggest PMMA particles are potential biomaterials to be used in the treatment of colon cancer.

Abbreviations: CO₂: carbon dioxide; DAPI: 4',6-diamidino-2-phenylindole; DMSO: dimethyl sulphoxide; DMEM: Dulbecco's Modified Eagle Medium; ELISA: enzyme-linked immunosorbent assay; FBS: foetal bovine serum; IU: international unit; MTT: (3 (4,5-dimethylthiazol-2-yl)-2,5-diphenyltetrazolium bromide; nm: nanometre; NPs: nanoparticles; OD: optical density; SEM: scanning electron microscopy; TEM: transmission electron microscopy; µg: microgram; µl: microlitre; FMSP-nanoparticles: fluorescent magnetic submicronic polymer nanoparticles

ARTICLE HISTORY

Received 23 December 2018
Revised 14 January 2019
Accepted 15 January 2019

KEYWORDS



Poly (methyl methacrylate); particles; colon cancer; TEM; SEM; anticancer agent

Background

Cancer treatment using nanoparticles (NPs) is very promising approach and different types and shapes of NPs have been tested in various cancers. Colon cancer is one of the leading causes of death around the world [1,2]. The cancer develops due to uncontrolled cell proliferation, and this condition is usually tackled by traditional chemotherapy, radiation and surgery interventions [3]. One of the major challenges of traditional approaches is that they produce poor therapeutic recovery, which is around 57% and generate serious side effects [4]. Owing to these issues, NPs have been considered as an alternate approach to treat and control the cancer. Because NPs are precise in targeting, with high biocompatibility, bioavailability and multifunctional capabilities [5–7]. Different size, structure and shapes of nanoparticles were

reported to cause cell death in cancer cells in both *in vitro* and *in vivo* studies [8–13].

In our pursuit to identify novel NPs for the treatment of cancer, we have decided to synthesize hydrophobic polymers such as poly (methyl methacrylate) (PMMA). Polymeric nano-carriers are found to be effective in safe drug delivery because its hydrophobic core which helps in the dissolution of hydrophobic drugs [14]. Among the different types of hydrophobic polymers, PMMA is widely used in drug delivery applications [15–18]. PMMA is basically biocompatible polyester with high resistance to chemical hydrolysis, and high drug permeability and most important is that it does not cause toxicity [19]. Recently, a few studies have been demonstrated that different forms and structures of PMMA possess anti-cancer properties [20–24]. There is no report on the effect of PMMA

CONTACT Firdos Alam Khan  fakhan@iau.edu.sa  Department of Stem Cell Biology, Institute for Research and Medical Consultations, Imam Abdulrahman Bin Faisal University, Post Box No. 1982, Dammam 31441, Saudi Arabia

© 2019 The Author(s). Published by Informa UK Limited, trading as Taylor & Francis Group.

This is an Open Access article distributed under the terms of the Creative Commons Attribution License (<http://creativecommons.org/licenses/by/4.0/>), which permits unrestricted use, distribution, and reproduction in any medium, provided the original work is properly cited.

(400–500 nm) on cancer cell viability and so considering various beneficial attributes of PMMA, we have decided to study the effect of PMMA on cancer cells. Here, we have studied the effects of PMMA on cancer cells by employing morphometric, MTT and DAPI. We have used different concentrations (1.0 µg/mL, 2.5 µg/mL, 5.0 µg/mL and 7.5 µg/mL) of PMMA and we have also evaluated their cytotoxic effects on normal healthy cells (human embryonic kidney, HEK-293) to check the specificity and selectivity of PMMA action. We have also performed wound healing experiments to check the weather PMMA can inhibit the cancer cell proliferation.

Methods

Synthesis and characterization of PMMA particles

Chemicals: Methyl methacrylate (MMA, Sigma-Aldrich, St. Louis, MO), methanol (VWR BDH Prolabo®) and potassium Persulphate (KPS, Sigma-Aldrich, St. Louis, MO, deionized water (DI)).

Preparation: Polymer methyl methacrylate (PMMA) was prepared as follows: in brief, 450 ml of water was added in the reactor and 500 ml of methanol was added were continuously stirred. Then 100 g of MMA were added to the mixture. The mixture was stirred at the speed of 120 RPM for 30 min. Then 0.2 g of the initiator (KPS) were solubilize in 50 ml water. This KPS initiator was then added to the mixture in the reactor to start polymerization. The polymerization was conducted for 20 h at 70 °C. The polymerization was investigated and found be 99.8% revealing the total consumption of MMA monomer.

Transmission electron microscopy (TEM) & scanning electron microscopy (SEM) analysis: The structure of PMMA was studied by SEM and the size was measured by using TEM. In brief, a drop of PMMA was deposited on TEM (Model-FEI, Morgagni 268, Czech Republic) grid supported by carbon film and it was operated at the voltage of 80 kV. We have taken several images with high magnifications to confirm the size of the PMMA and for that purpose Gatan digital micrograph software was applied to measure the size of the PMMA. Furthermore, the complete morphology of PMMA was inspected by SEM (Model-FEI, Inspect-S50, Moravia, Czech Republic) where SEM was operated at 20 kV.

Zeta sizer: The size distribution pattern of PMMA particles were analyzed by Zeta sizer (NANO-ZS, Malvern Instruments, Worcestershire, UK). A small drop of the sample was dispersed in 1 mM NaCl. The measurement was repeated for three times. The PMMA particles were assessed by Fluorescence Spectrophotometer (LS50 System, Perkin Elmer, Waltham, MA). The structural appearance and morphology of PMMA particles was studied by SEM (FEI, Czech Republic), and the size of PMMA was measured by TEM (FEI, Czech Republic), respectively.

Hydrodynamic size analysis: PMMA latex particle size was calculated by using quasi elastic light scattering (QELS) using nano-ZS (Malvern Instrument, Worcestershire, UK). The mean hydrodynamic diameter (DH) was calculated from the diffusion co-efficient measurement, which in the high dilution

limits the negligible particle–particle interactions, is calculated by using the Stokes–Einstein equation:

$$D = \frac{kT}{3\pi\eta D_h}$$

where D is the diffusion coefficient, k is the Boltzmann constant, T is the absolute temperature and η is the viscosity of the medium.

Cell culture and treatment of PMMA particles

We have taken human colorectal carcinoma (HCT-116) cells for testing PMMA. The HCT-116 cells with a concentration of $2 \times 10^5/\text{cm}^2$ were first seeded in DMEM media, (1%) L-glutamine, (10%) FBS, (1%) selenium chloride, (1%) penicillin and (1%) streptomycin. They were grown in the CO₂ incubator (Thermoscientific, Waltham, MA) at 37 °C. The cells were grown in 96 well plate and we have added approximately 200 µl media in each well. When the cells become 80% confluence, they were treated with different concentrations 1.0 µg/mL, 2.5 µg/mL, 5.0 µg/mL and 7.5 µg/mL of PMMA. The treated cell morphology was monitored after 24 h and 48 h of PMMA treatments. We have also tested the PMMA on human embryonic kidney cells (HEK-293), which are normal healthy cells. We have taken triplicate samples for the statistical calculations.

Cancer cell morphology by light microscopy

After 48 h of PMMA treatments, both healthy cells (HEK-293) and cancerous cells (HCT-116) cells were observed under an inverted microscope (TS100F Eclipse, Nikon, Tokyo, Japan) to examine the morphological and anatomical changes. We have first analysed the effects on HEK-293 and then we have analysed on HCT-116 cells, respectively. Each sample was observed (100×, 200× and 400×) magnifications. The cell morphology of PMMA-treated and non-PMMA-treated cells examined and compared.

Cancer cell viability by MTT assay

Both HEK-293 and HCT-116 cells were grown in DMEM, FBS (10%), (1%) penicillin and (1%) streptomycin in the CO₂ incubator at the temperature (37 °C) and CO₂ (5%) conditions. The cells were first plated with a density of 9.0×10^4 cells/well into 96-well plates. Once cells reached to 80% confluency, cells were treated (7.5 µg/mL) with PMMA nanoparticles. In control group, no PMMA was added. After 48 h of treatment, 5.0 mg/mL of MTT was added and incubated for 4 h. Finally, the media was changed and 100 µl of DMSO was added in each well and were taken for measuring O.D. through ELISA plate reader (Biotek Instruments, Winooski, VT). The samples were read at the wavelength of 570 nm wavelength. The cell viability (%) was calculated as per given formula:

$$\begin{aligned} &\% \text{ of Cell viability} \\ &= \frac{\text{Optical density (O.D.) of PMMA-treated cells}}{\text{Optical density (O.D.) of control cells}} \times 100 \end{aligned}$$

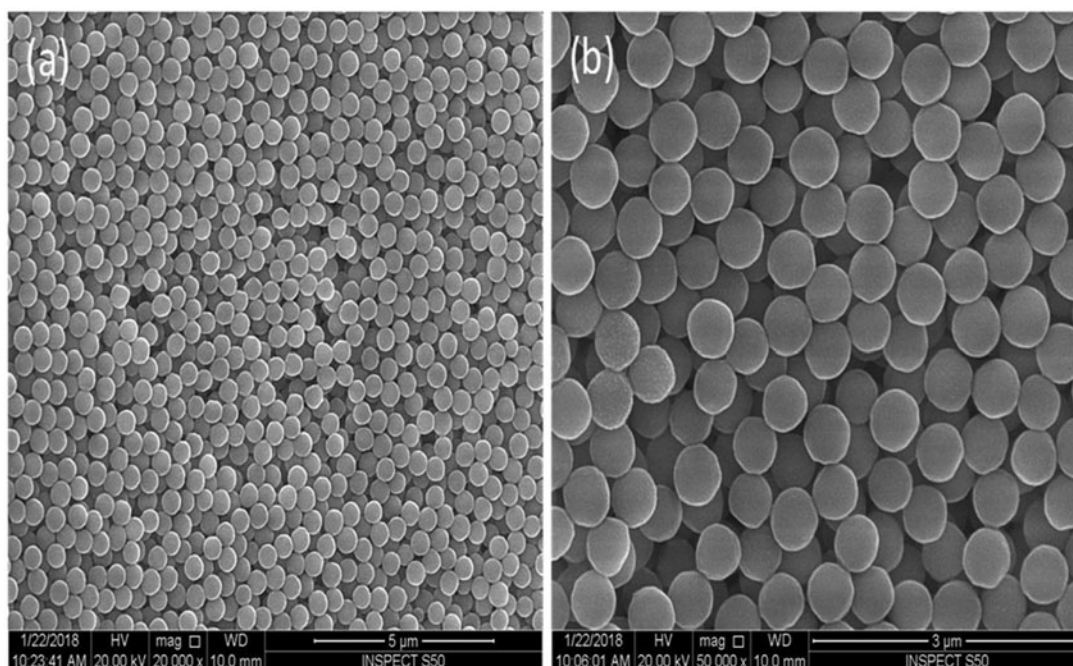


Figure 1. SEM surface morphology of PMMA particles at two magnifications, 20,000 \times (a) and 50,000 \times (b). The particles show uniform morphology with spherical shape and a narrow size distribution.

Wound healing by scratch assay

The scratch assay has been performed as per previous report [25]. In brief, HCT-116 cells were cultured in a 6-well plate and once they reached to 90% confluency, they were processed for wound healing assay. To make a scratch in the cell culture, we have taken sterilized glass pipette and tip of the glass pipette was used to scrape the cells in a straight line to create an empty gap. The cell debris was then removed by washing the cells with a culture medium and then replaced with 2 mL of fresh medium. Thereafter, we have added 7.5 $\mu\text{g/mL}$ of PMMA and in the control group we did not add the PMMA. After 24 h, scratch line was observed to check any morphological changes.

Nuclear morphology detection by DAPI stain

DAPI staining assay was carried out to examine the effect of PMMA on both HEK-293 and HCT-116 cell nucleus. Both HEK-293 and HCT-116 cells were divided into two groups, one was control (without PMMA treatment) and another one was PMMA-treated groups. After 48 h of treatment, both control and PMMA-treated groups were pre-treated with ice-cold (4%) paraformaldehyde. Then cells were treated with (0.1%) Triton X-100 in phosphate-buffered saline (PBS) for 5 min for cell membrane permeabilization. Both control and PMMA-treated cells were stained with DAPI (1 $\mu\text{g/mL}$) prepared in PBS for 5 min in the dark environment. Finally, the cells were washed with (0.1%) Triton X-100 prepared in PBS. The nuclear morphology of both control and PMMA-treated cells was examined under confocal scanning microscope (Zeiss, Berlin, Germany) equipped with digital camera.

Statistical evaluation

Data in the graphs were presented as mean \pm standard deviation which was obtained from three experiments. Statistical analysis was performed using ANOVA followed by Dunnett's *post hoc* test of Graph-Pad Prism Software (GraphPad Software, La Jolla, CA). The p value ($*p < .05$) was considered as statistically significant.

Results

SEM & TEM characterization of PMMA particles

The structural appearance of PMMA particles was determined by SEM and TEM methodologies. SEM surface morphology of PMMA particles is shown in Figure 1(a,b) with 20,000 \times and 50,000 \times magnifications. The particles show uniform morphology with spherical shape and a narrow size distribution.

We have analysed the size of PMMA particles using TEM. TEM images at two different magnifications displaying the spherical nature of the particles (Figure 2(a,b)). The particles show a narrow size distribution. Intensity profile extracted from the selected nanoparticles as highlighted by the green line in the image. The diameter of the particles is around 480 nm (Figure 2(c)) and the size histogram of the PMMA particles showing the size distribution, more than 50 particles were measured for this analysis using Gatan digital micrograph software (Figure 2(d)). The average diameter of the nanoparticles was estimated around 470 ± 4 nm.

The hydrodynamic size of the prepared PMMA latex particles was investigated in 1 mM NaCl solution. The hydrodynamic size deduced from Stokes–Einstein equation was found to be 606 nm with narrow size distribution as illustrated in Figure 3.

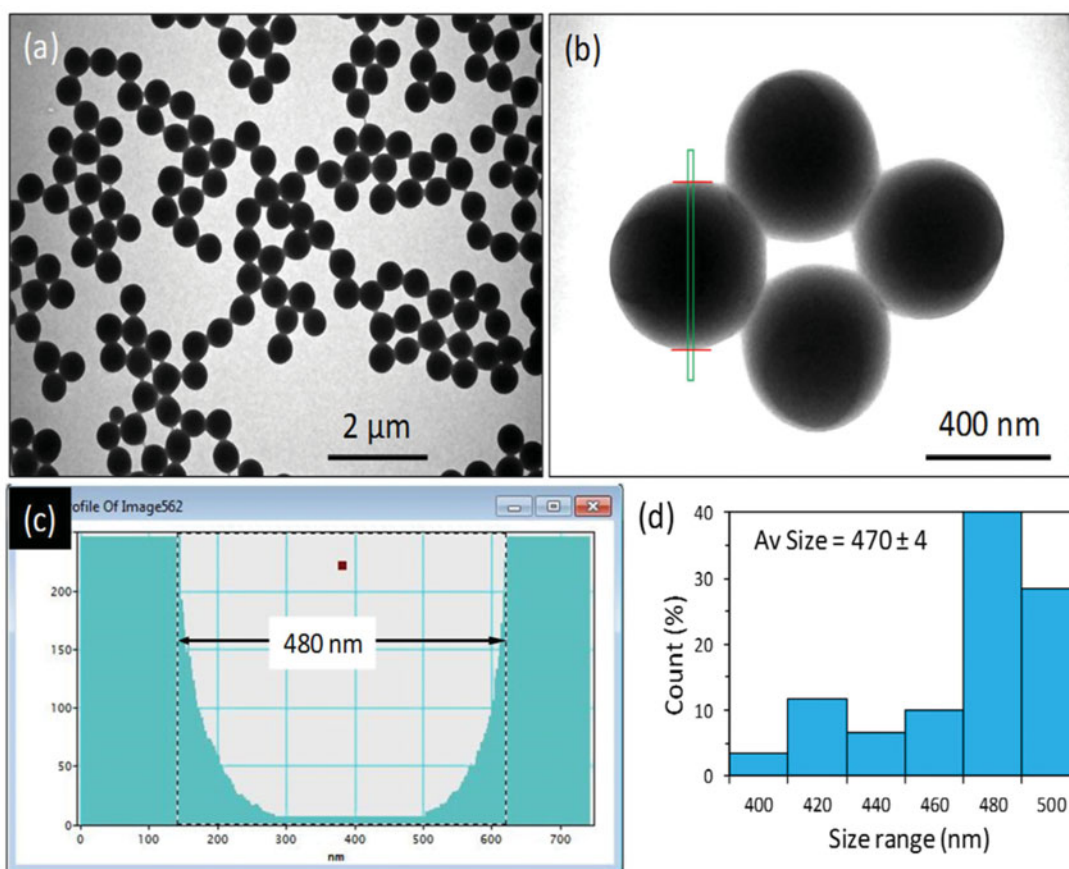


Figure 2. Morphology and size analysis of the polymethyl methacrylate (PMMA) nanoparticles. (a,b) TEM images at two different magnifications displaying the spherical nature of the particles. The particles show a narrow size distribution. (c) Intensity profile extracted from the selected nanoparticles as highlighted by green line in the image. The diameter of the particles is around 480 nm. (d) Size histogram of the PMMA particles showing the size distribution, more than 50 particles were measured for this analysis using Gatan digital micrograph software. The average diameter of the nanoparticles was estimated around 470 ± 4 nm.

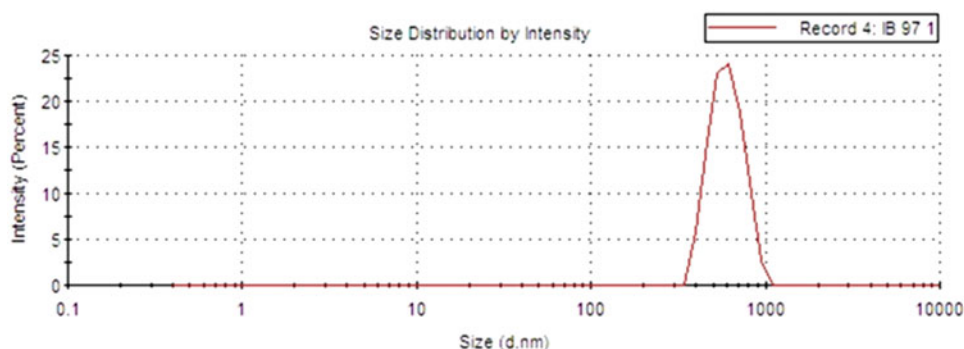


Figure 3. Hydrodynamic size distribution of the prepared PMMA latex particles. The hydrodynamic size deduced from Stokes-Einstein equation was found to be 606 nm with narrow size distribution.

Cell morphology

The impact of PMMA particles was evaluated by microscopic observations.

24 h post-treatment: The treatments of $5.0 \mu\text{g/mL}$ and $7.5 \mu\text{g/mL}$ showed no anatomical and morphological changes in HEK-293 cells. The cell membrane and nucleus appeared healthy and normal (Figure 4(a-c)). Whereas the treatments of $5.0 \mu\text{g/mL}$ and $7.5 \mu\text{g/mL}$ on HCT-116 showed nuclear condensation of cancerous cells was observed (Figure 4(d,e,f)) in

HCT-116 cells, whereas no nuclear condensation was observed in healthy cells (HEK-293) (Figure 4(a-c)).

48 h post-treatment: The treatments of $5.0 \mu\text{g/mL}$ and $7.5 \mu\text{g/mL}$ showed no anatomical and morphological changes in HEK-293 cells. The cell membrane and nucleus appeared healthy and normal (Figure 5(a-c)). Whereas the treatments of $5.0 \mu\text{g/mL}$ and $7.5 \mu\text{g/mL}$ on HCT-116 showed nuclear condensation of cancerous cells was observed (Figure 5(d-f)) in HCT-116 cells, whereas no nuclear condensation was observed in healthy cells (HEK-293) (Figure 5(a-c)).

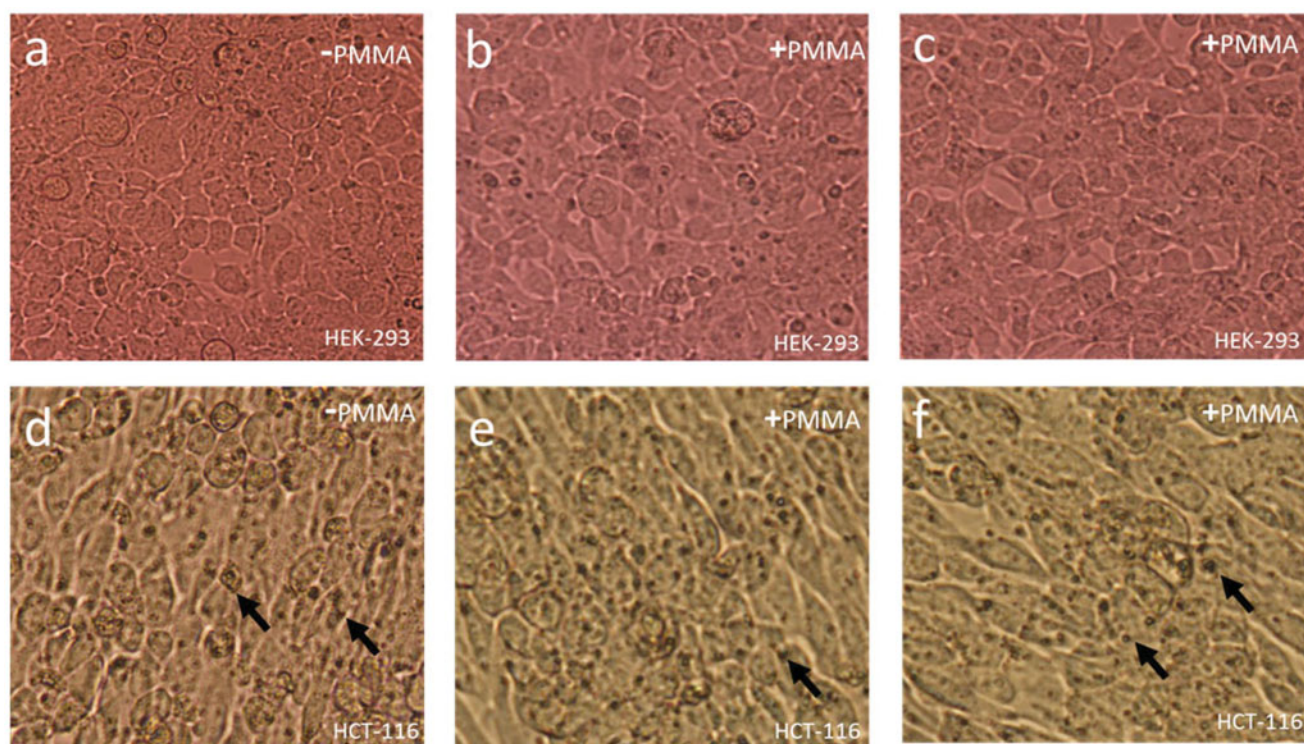


Figure 4. Cell Morphology of HEK-293 and HCT-116 cells after 24 h of treatment of PMMA: (a) control, (b) 5.0 µg/mL and (c) 7.5 µg/mL of HEK-293 cells. (d) Control, (e) 5.0 µg/mL and (f) 7.5 µg/mL of HEK-293 cells. Nuclear condensation (arrows) (400× magnifications).

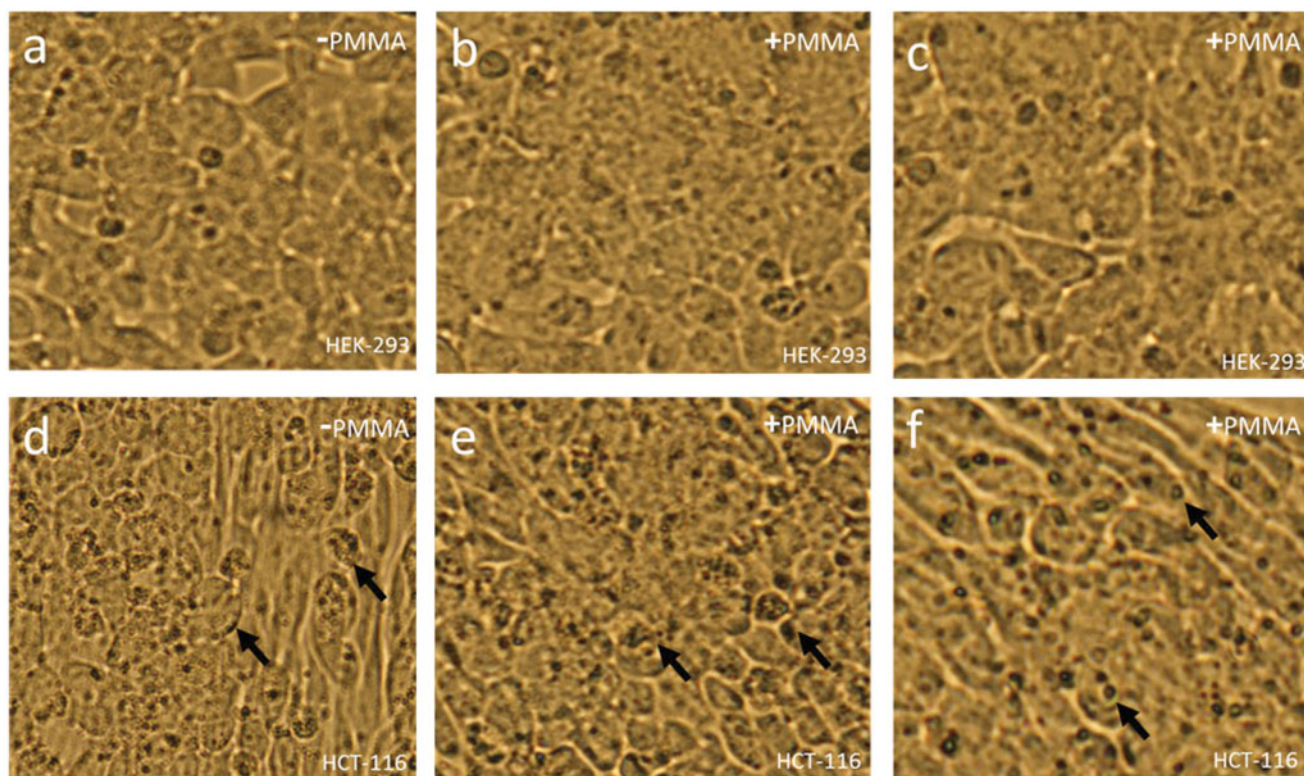


Figure 5. Cell Morphology of HEK-293 and HCT-116 cells after 48 h of treatment of PMMA: (a) control, (b) 5.0 µg/mL and (c) 7.5 µg/mL of HEK-293 cells. (d) Control, (e) 5.0 µg/mL and (f) 7.5 µg/mL of HEK-293 cells. Nuclear condensation (arrows). (400× magnifications).

Cell viability assay by MTT

The cell viability test was done post-PMMA particle treatments using both HEK-293 and HCT-116 cells. We have used

MTT assay with different concentrations (1.0 µg/mL, 2.5 µg/mL, 5.0 µg/mL and 7.5 µg/mL) of PMMA particles for 48 h. The treatment of dose 1.0 µg/mL on HCT-116 cells showed moderate decrease (82%) in cell viability with compares to control

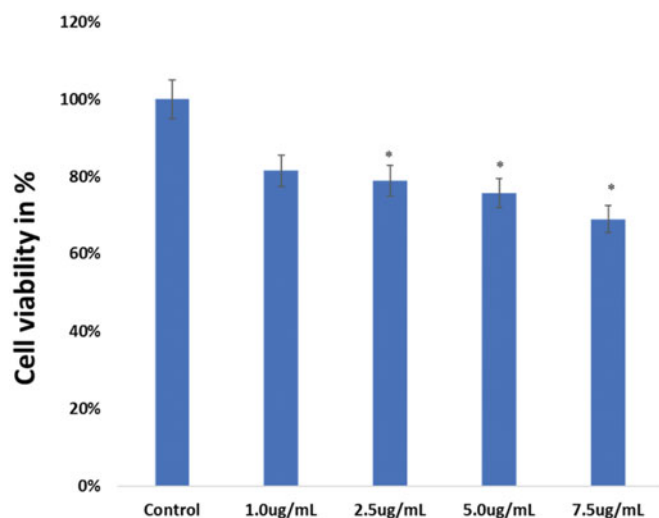


Figure 6. Cell viability analysis. HCT-116 cells were treated with PMMA (1 µg/mL, 2.5 µg/mL, 5.0 µg/mL and 7.5 µg/mL) for 48 h and then processed for MTT analysis. Data are the means \pm SD of three different experiments. Difference between two treatment groups was analysed by Student's *t* test where (**p* < .05), *p* values were calculated by Student's *t* test.

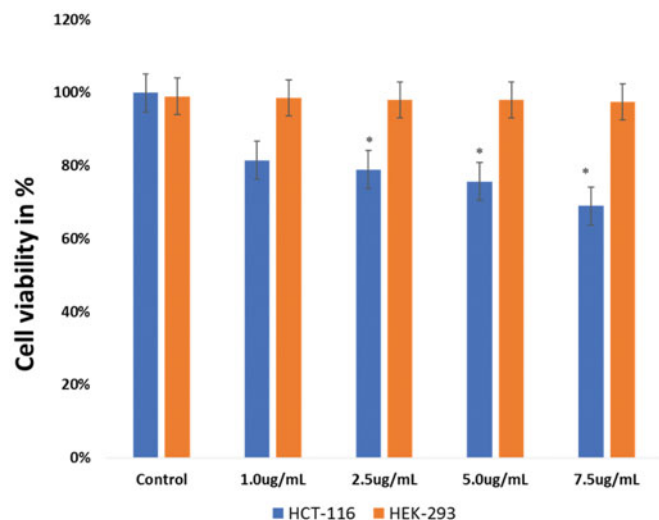


Figure 7. Cell viability analysis: PMMA (1 µg/mL, 2.5 µg/mL, 5.0 µg/mL and 7.5 µg/mL) were treated to HCT-116 and HEK-293 cells for 48 h and processed for MTT assay. Data are the means \pm SD of three different experiments. Difference between two treatment groups was analysed by Student's *t* test where (**p* < .05), *p* values were calculated by Student's *t* test.

cells (Figures 6 and 7), whereas the treatments of dosages (2.5 µg/mL, 5.0 µg/mL and 7.5 µg/mL) showed steadily decrease in the cell viability to 78.91%, 75.66% and 68.96% (Figures 6 and 7). When PMMA particles were treated to HEK-293 cells, we did not find any changes in the cell viability and it remained same in all dosages (1.0 µg/mL, 2.5 µg/mL, 5.0 µg/mL and 7.5 µg/mL) (Figure 7).

Wound healing assay

With a view to check whether PMMA produce any effect on cancer cells in wound healing capabilities. We have found PMMA particle treatment almost stopped the wound healing process and no cell proliferation was observed in the scratch area (Figure 7(c, d)), with comparable non-PMMA-treated cells

(Figure 8(b,c)). However, cells in which no PMMA was added to show proliferation of cancer cells (Figure 8(a, b)).

Cancer cell nuclear morphology by DAPI stain

The cancer cell nuclear morphological changes post-PMMA treatments were examined to understand whether the observed cell death is due to programmed cells death (apoptosis) or necrosis (Figure 9). We observed that PMMA-treatment caused significant loss of nuclear staining in the HCT-116 cells (Figure 9(d)) when compared with the non-PMMA-treated control (Figure 9(c)). Furthermore, PMMA-treatment did not cause any loss of nuclear staining in HEK-293 cells (Figure 9(b)) when compared with control (Figure 9(a)) which suggests that PMMA selectively target the cancerous cells (HCT-116) and induced cancer cell death.

The effects of PMMA particles on both HCT-116 and HEK-293 cells are diagrammatically depicted in Figure 10, where Figure 10(a) shows the structure of PMMA particles through SEM, Figure 10(b) shows the treatment of PMMA particles with HCT-116 and HEK-293 cells in the Petri dishes and Figure 10(c) shows the PMMA-treated HCT-116 cancer cells undergoing cell death, whereas PMMA-treated HEK-293 cells remain unaffected.

Discussion

The structure of PMMA was studied by SEM and the size was measured by using TEM. The size distribution pattern of PMMA particles was analysed by Zeta sizer and the PMMA particle size was calculated by using QELS. The particles size was found to be 606 nm as per QELS analysis, whereas it was 480 nm as TEM analysis. The observed difference between TEM and QELS techniques can be attributed to these factors. For example, TEM is performed on dried sample whereas QELS is performed in aqueous medium, secondly more the particle size is close to the wavelength of the beam (which is 632 nm for the used equipment), more the sensitivity is lost, and third most important factors is polymerization. QELS was performed in the mixture of water and methanol and the solid content was 10% w/v, then we cannot exclude the presence of few aggregates which may enlarge the hydrodynamic particle size measured by QELS even if the zeta potential is -45 mV revealing the good colloidal stability of PMMA particles in water since the zeta potential has been measured in 1 mM NaCl solution.

Our findings showed that PMMA particles inhibit the cancer cell viability in a dose dependent manner. The treatment of dose (1.0 µg/mL) on HCT-116 cells showed moderate decrease (82%) in cell viability with compares to control cells, whereas the treatments of dosages (2.5 µg/mL, 5.0 µg/mL and 7.5 µg/mL) showed steadily decrease in the cell viability to 78.91%, 75.66% and 68.96%. This is the first report in which we have demonstrated the use of only PMMA for the cancer treatments. Whereas there are few reports where PMMA has been conjugated with other particles or drug molecules to treat cancer cells. For example, core shell PMMA particles were covalently functionalized with porphyrin showed

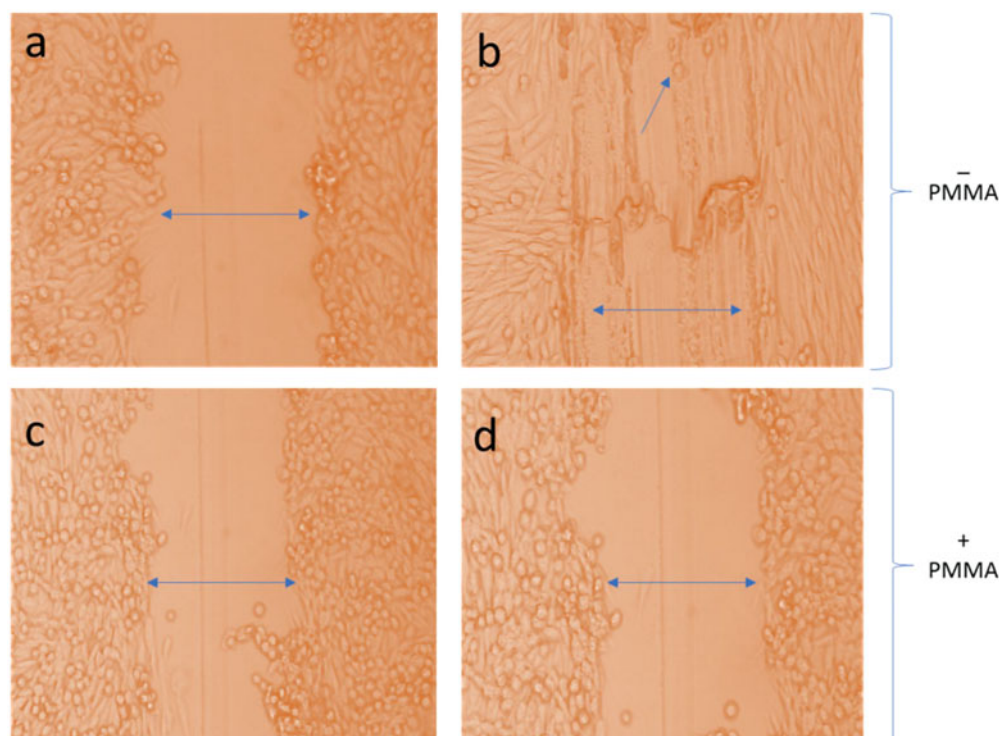


Figure 8. Effect of PMMA on wound healing. Wound healing assays of PMMA was performed in HCT-116 cells. These are representative photographs of (a) non-treated HCT-116 with scratch 0 h, (b) non-treated HCT-116 cells after 24 h, (c) PMMA-treated cells (7.5 $\mu\text{g/mL}$) 0 h and (d) PMMA-treated cells (7.5 $\mu\text{g/mL}$) 24 h. Figure (b) shows healing of cells after 24 h, whereas (d) shows no-healing after 24 h. 400 \times magnifications.

anticancer action (Ballestri et al., 201). PMMA particles have been shown to inhibit metastatic cancer cells [22]. Moreover, curcuminoid-loaded PMMA particles have been reported to inhibit the cancer cell proliferation [23]. In another report, PMMA conjugated with arginine, glycine, aspartic acid (RGD) – peptide sequence showed strong anti-cancer activities [21]. In our studies, we report for the first-time effect of PMMA particles on human colorectal cells. As we were keen to study the human colorectal cancer, we have selected human colorectal carcinoma cells (HCT-116) to assess anti-cancer properties of PMMA nanoparticles. HCT-116 cells have been widely used as a model for testing the anticancer drugs [25–32].

We were interested to examine the effect of PMMA on cancer cell morphology. We have examined the cancer cells (HCT-116) and normal cells (HEK-293) under microscope and evaluated and compared the morphological changes. The treatment of PMMA on HEK-293 cells showed no anatomical and morphological changes and the cell membrane and nucleus appeared healthy and normal. Whereas PMMA treatment showed a drastic change in cell structure and membrane. Morphological findings are in agreement with MTT assay results, as many cancer cells were found to be dead post PMMA treatment. We have also examined the nuclear morphological changes after treating the cells with PMMA to understand whether the observed cell death is due to programmed cells death (apoptosis) or necrosis. We observed that PMMA-treatment caused significant loss of nuclear staining in the HCT-116 cells when compared with the non-PMMA-treated control. Furthermore, PMMA-treatment did not cause any loss of nuclear staining in HEK-293 cells when compared with control which suggests that PMMA selectively

target the cancerous cells (HCT-116) and induced cancer cell death. While we do not the molecular mechanism of PMMA induced cell death, it would be interesting to study molecular mechanisms of PMMA mediated cell death in the HCT-116 cells.

To check the specificity of PMMA on cancer cells, we have used two different cells HCT-116 (colon cancer) and HEK-293 (normal cells) and compared the response. We have found that PMMA inhibited the HCT-116 cell proliferation in a dose dependent manner, whereas it did not cause any effects on HEK-293 cells. These results suggest that PMMA has strong specificity against cancer cells. Our results are also in line with previous reports which showed that PMMA do not cause any toxicity to normal cells [19].

We have also calculated the size of the PMMA particles to know how do PMMA particles produce lethal effects on the cancer cells. We have done SEM and TEM data analysis, which revealed that PMMA particles have the size ranging from 400 to 500 nm. While we do not know the mechanism of internalization of PMMA particles in cancer cells, but the possibility of endocytosis of PMMA particles cannot be ruled out. Previously, we have shown the successful internalization of FMSP-nanoparticles (300–400 nm) inside cancer cells, which induced the cancer cell death [27]. There are several reports of internalization of nanoparticles [33,34,35] which led to cell death. It would be interesting to study the how PMMA enters the cancer cells and induce the cell death by using *in vitro* and animal models.

It has been confirmed that metastasis is serious problem that caused enormous cancer deaths around the world [36,37]. Hence, targeting the migratory pattern of cancer cells

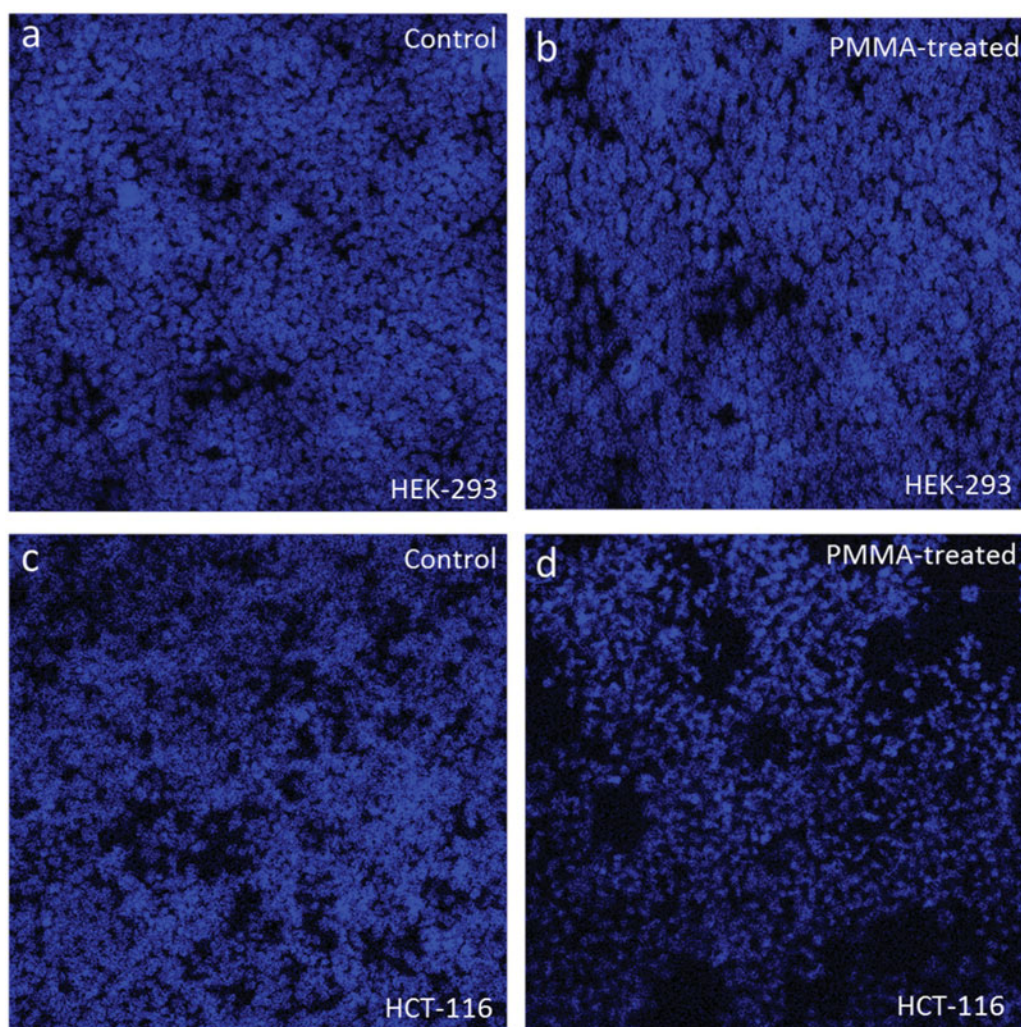


Figure 9. (a–d) Confocal microscopic images of HEK-293 and HCT-116 cells stained with DAPI: Figures (a) and (c) are control cells (without PMMA treatment), whereas (b) and (d) treated with PMMA (7.5 $\mu\text{g}/\text{mL}$) for 48 h. There is no cell death in PMMA-treated HEK-293 cells (d), whereas there is a significant loss of HCT-116 cells treated with PMMA when compared with control cells. 200 \times magnifications.

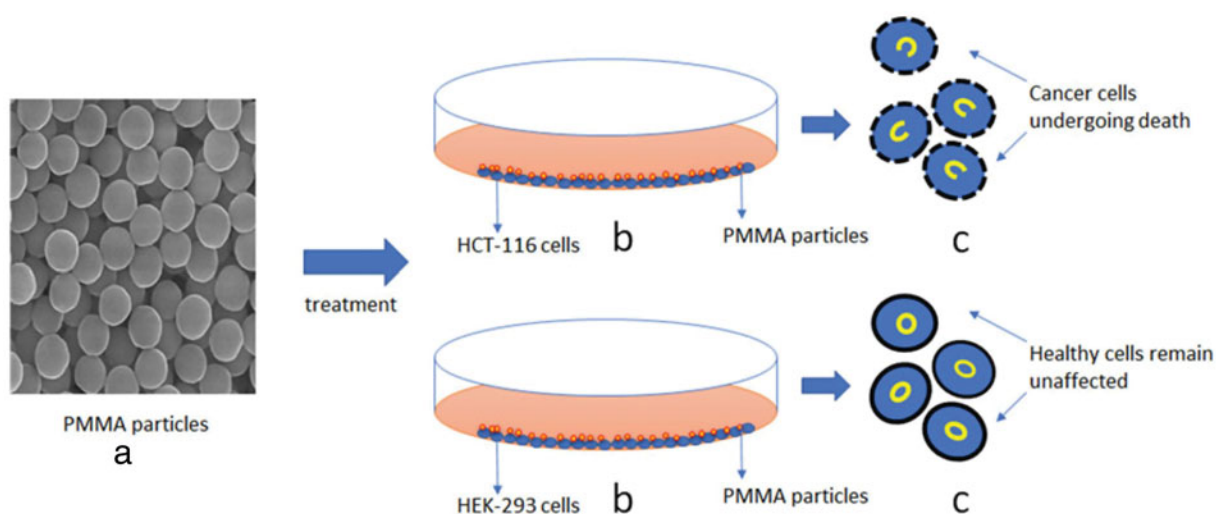


Figure 10. (a–c) Schematic representation of treatment of PMMA particles on cancer cells: (a) structure of PMMA particles through scanning electron microscope with 50,000 \times magnification, (b) treatment of PMMA particles with HCT-116 and HEK-293 cells in the Petri dishes and (c) showing PMMA-treated HCT-116 cancer cells undergoing membrane disruption, and nuclear condensation and augmentation, whereas PMMA-treated HEK-293 cells remain unaffected.

would be an effective approach to manage or control cancer growth. Consequently, we examined whether PMMA inhibit the migration of colon cancer cells. We have found that treatment of PMMA inhibited the migration of cancer cells, which was studied for 48 h. However, cancer cells in which we did not add PMMA showed strong proliferation of cancer cells. The wound healing experiments suggest that PMMA inhibited cancer cells proliferation, whereas positive cancer cell proliferation was observed in the non-PMMA-treated cells. The results suggest that PMMA is highly specific in targeting the cancer cells. Similar reports were reported, where hetero-metallic Au@Pt-nanoseeds (NSs) displayed inhibitory activity against the migrating cancer cells [36,38].

Conclusion

We report that PMMA particles inhibited the cancer cell viability in a dose-dependent manner. The lower dose (1.0 µg/mL) showed a moderate decrease in cancer cell viability, whereas higher dosages (2.5 µg/mL, 5.0 µg/mL and 7.5 µg/mL) showed steadily decrease in the cancer cell viability. We report that PMMA is highly selective to cancerous cells (HCT-116), as we did not find any action on the normal healthy cells (HEK-293). Interestingly, we have found that cancer cell death after PMMA-treatment is due to nuclear disintegration as observed by DAPI stained confocal microscopy analysis. PMMA induce nucleus condensation and augmentation which is responsible for the cell death. We also report PMMA action is highly selective, as both HEK-293 cells and scratch experiments confirm that PMMA particles selectively targeted the cancerous cells. Based on the results, we suggest that PMMA particles are potential biomaterials for the cancer treatments.

Authors' consent for publication

This manuscript is approved by all authors for the submission.

Availability of data and material

The research data is available upon a request.

Acknowledgements

Authors are thankful to Institute for Research & Medical Consultations (IMRC), Imam Abdulrahman Bin Faisal University, Dammam, Saudi Arabia for providing the laboratory facilities and equipment to perform the experiments. The authors are also thankful to Mr Abdullah Buhaimeid (volunteer) and Mr Dioneicio Jr Bagon Dela Roca for performing cell culture and bioassay related work. We appreciate the help of Dr Khaldoon M. Alsamman, Clinical Laboratory Science, College of Applied Medical Science, Imam Abdulrahman Bin Faisal University, Dammam, Saudi Arabia, for providing HCT-116 and HEK-293 cell lines.

Disclosure statement

No potential conflict of interest was reported by the authors.

ORCID

Firdos Alam Khan  <http://orcid.org/0000-0002-6892-1530>

References

- [1] Ninon V, Lefebvre T, Yazidi-Belkoura IE. Drug resistance related to aberrant glycosylation in colorectal cancer. *Oncotarget*. 2018;9: 1380–1402.
- [2] Siegel R, Ma J, Zou Z, et al. Cancer statistics, 2014. *CA Cancer J Clin*. 2014;64:9–29.
- [3] Smalley KS, Herlyn M. Towards the targeted therapy of melanoma. *Mini Rev Med Chem*. 2006;6:387–393.
- [4] Yaffee P, Osipov A, Tan C, et al. Review of systemic therapies for locally advanced and metastatic rectal cancer. *J Gastrointest Oncol*. 2015;6:185–200.
- [5] Afrimzon E, Deutsch A, Shafran Y, et al. Intracellular esterase activity in living cells may distinguish between metastatic and tumor-free lymph nodes. *Clin Exp Metastasis*. 2008;25:213–224.
- [6] Aftab S, Shah A, Nadhman A, et al. Nanomedicine: an effective tool in cancer therapy. *Int J Pharm*. 2018;540:132–149.
- [7] Zhao J, Castranova V. Toxicology of nanomaterials used in nanomedicine. *J Toxicol Environ Health B Crit Rev*. 2011;14:593–632.
- [8] Gottlieb E, Armour SM, Harris MH, et al. Mitochondrial membrane potential regulates matrix configuration and cytochrome c release during apoptosis. *Cell Death Differ*. 2003;10:709–717.
- [9] Jiang H, Shi X, Yu X, et al. Hyaluronidase enzyme-responsive targeted nanoparticles for effective delivery of 5-fluorouracil in colon cancer. *Pharm Res*. 2018;35:73.
- [10] Pati R, Das I, Mehta RK, et al. Zinc-oxide nanoparticles exhibit genotoxic, clastogenic, cytotoxic and actin depolymerization effects by inducing oxidative stress responses in macrophages and adult mice. *Toxicol Sci*. 2016;150:454–472.
- [11] Unfried K, Albrecht C, Klotz LO, et al. Cellular responses to nanoparticles: target structures and mechanisms. *Nanotoxicology*. 2007; 1:52–71.
- [12] Wang H, Wick RL, Xing B. Toxicity of nanoparticulate and bulk ZnO, Al₂O₃ and TiO₂ to the nematode *Caenorhabditis elegans*. *Environ Pollut*. 2009;157:1171–1177.
- [13] Wood A, Schneider J, Shilatifard A. Cross-talking histones: implications for the regulation of gene expression and DNA repair. *Biochem Cell Biol*. 2005;83:460–467.
- [14] Mukherjee A, Vishwanatha JK. Formulation, characterization and evaluation of curcumin-loaded PLGA nanospheres for cancer therapy. *Anticancer Res*. 2009;29:3867–3876.
- [15] Cyphert EL, Learn GD, Hurley SK, et al. An additive to PMMA bone cement enables postimplantation drug refilling, broadens range of compatible antibiotics, and prolongs antimicrobial therapy. *Adv Healthcare Mater*. 2018;7:e1800812.
- [16] Feuser PE, Arévalo JM, Junior EL, et al. Increased cellular uptake of lauryl gallate loaded in superparamagnetic poly(methyl methacrylate) nanoparticles due to surface modification with folic acid. *J Mater Sci Mater Med*. 2016;27:185. Epub 2016 Oct 27.
- [17] Graça D, Louro H, Santos J, et al. Toxicity screening of a novel poly(methylmethacrylate)-Eudragit nanocarrier on L929 fibroblasts. *Toxicol Lett*. 2017;276:129–137.
- [18] Neumann SE, Chamberlayne CF, Zare RN. Electrically controlled drug release using pH-sensitive polymer films. *Nanoscale*. 2018;10: 10087–10093.
- [19] Elvira C, Fanovich A, Fernandez M, et al. Evaluation of drug delivery characteristics of microspheres of PMMA-PCL-cholesterol obtained by supercritical-CO₂ impregnation and by dissolution-evaporation techniques. *J Control Release*. 2004;99:231–240.
- [20] Ballestri M, Caruso E, Guerrini A, et al. Core-shell poly-methyl methacrylate nanoparticles covalently functionalized with a non-symmetric porphyrin for anticancer photodynamic therapy. *J Photochem Photobiol B*. 2018;186:169–177.

- [21] Gibbens-Bandala BV, Ocampo-García BE, Ferro-Flores G, et al. Multimeric system of RGD-grafted PMMA-nanoparticles as a targeted drug- delivery system for paclitaxel. *Curr Pharm Des.* 2017; 23:3415–3422.
- [22] Nikshoar MS, Khosravi S, Jahangiri M, et al. Distinguishment of populated metastatic cancer cells from primary ones based on their invasion to endothelial barrier by biosensor arrays fabricated on nanoroughened poly(methyl methacrylate). *Biosens Bioelectron.* 2018;118:51–57.
- [23] Sahu A, Solanki P, Mitra S. Curcuminoid-loaded poly(methyl methacrylate) nanoparticles for cancer therapy. *IJN.* 2018;13:101–105.
- [24] Mendes AN, Filagueiras LA, Siqueira MRP, et al. Encapsulation of Piper cabralanum (Piperaceae) nonpolar extract in poly(methyl methacrylate) by miniemulsion and evaluation of increase in the effectiveness of antileukemic activity in K562 cells. *Int J Nanomed.* 2017;12:8363–8373.
- [25] Liang CC, Park AY, Guan JL. In vitro scratch assay: a convenient and inexpensive method for analysis of cell migration in vitro. *Nat Protoc.* 2007;2:329–333.
- [26] Asif M, Shafaei A, Abdul Majid AS, et al. Mesua ferrea stem bark extract induces apoptosis and inhibits metastasis in human colorectal carcinoma HCT 116 cells, through modulation of multiple cell signalling pathways. *Chin J Nat Med.* 2017;15:505–514.
- [27] Khan FA, Akhtar S, Almohazey D, et al. Fluorescent magnetic sub-micronic polymer (FMSP) nanoparticles induce cell death in human colorectal carcinoma cells. *Artif Cells Nanomed Biotechnol.* 2018;25:1–7.
- [28] Matsuoka K, Kobunai T, Nukatsuka M, et al. Improved chemoradiation treatment using trifluridine in human colorectal cancer cells in vitro. *Biochem Biophys Res Commun.* 2017;494:249–255.
- [29] Mazewski C, Liang K, Gonzalez de Mejia E. Comparison of the effect of chemical composition of anthocyanin-rich plant extracts on colon cancer cell proliferation and their potential mechanism of action using in vitro, in silico, and biochemical assays. *Food Chem.* 2018;242:378–388.
- [30] Sinha A, Banerjee K, Banerjee A, et al. Induction of apoptosis in human colorectal cancer cell line, HCT-116 by a vanadium-Schiff base complex. *Biomed Pharmacother.* 2017;92:509–518.
- [31] Sudeep HV, Gouthamchandra K, Venkatesh BJ, et al. Viwithan, a Standardized Withania somnifera root extract induces apoptosis in murine melanoma cells. *Pharmacogn Mag.* 2018;13:S801–S806.
- [32] Zeng M, Zhu L, Li L, et al. miR-378 suppresses the proliferation, migration and invasion of colon cancer cells by inhibiting SDAD1. *Cell Mol Biol Lett.* 2017;22:12. eCollection 2017. PMID: 28725241
- [33] Chen H, Zhang T, Zhou Z, et al. Enhanced uptake and cytotoxicity of folate-conjugated mitoxantrone-loaded micelles via receptor up-regulation by dexamethasone. *Int J Pharm.* 2013;448:142–149.
- [34] Serpe L, Gallicchio M, Canaparo R, et al. Targeted treatment of folate receptor-positive platinum-resistant ovarian cancer and companion diagnostics, with specific focus on vintafolide and etarfolatide. *Pharmgenomics Pers Med.* 2014;7:31–42.
- [35] Thomas TP, Huang B, Choi SK, et al. Polyvalent dendrimer-methotrexate as a folate receptor-targeted cancer therapeutic. *Mol Pharm.* 2012;9:2669–2676.
- [36] Bianco FJ Jr, Gervasi DC, Tiguert R, et al. Matrix metalloproteinase-9 expression in bladder washes from bladder cancer patients predicts pathological stage and grade. *Clin Cancer Res.* 1998;4: 3011–3016.
- [37] Davies B, Waxman J, Wasan H, et al. Levels of matrix metalloproteinases in bladder cancer correlate with tumor grade and invasion. *Cancer Res.* 1993;53:5365–5369.
- [38] Lee EJ, Lee SJ, Kim S, et al. Interleukin-5 enhances the migration and invasion of bladder cancer cells via ERK1/2-mediated MMP-9/ NF- κ B/AP-1 pathway: involvement of the p21WAF1 expression. *Cell Signal.* 2013;25:2025–2038.